

AperTO - Archivio Istituzionale Open Access dell'Università di Torino

As-bearing new mineral species from Valletta mine, Maira Valley, Piedmont, Italy: II. Braccoite, $\text{NaMn}_2+5[\text{Si}_5\text{AsO}_{17}(\text{OH})](\text{OH})$, description and crystal structure

This is the author's manuscript

Original Citation:

Availability:

This version is available <http://hdl.handle.net/2318/1508613> since 2015-12-02T14:53:28Z

Published version:

DOI:10.1180/minmag.2015.079.1.14

Terms of use:

Open Access

Anyone can freely access the full text of works made available as "Open Access". Works made available under a Creative Commons license can be used according to the terms and conditions of said license. Use of all other works requires consent of the right holder (author or publisher) if not exempted from copyright protection by the applicable law.

(Article begins on next page)



UNIVERSITÀ DEGLI STUDI DI TORINO

This is an author version of the contribution published on:

Questa è la versione dell'autore dell'opera:
Mineralogical Magazine, 79(1), 171-189.2015
<http://dx.doi.org/10.1180/minmaq.2015.07>

The definitive version is available at:

La versione definitiva è disponibile alla URL:
<http://www.minersoc.org/minmaq.html>

1
2
3
4
5
6
7
8
9
10
11
12
13
14
15
16
17
18
19
20
21
22
23
24

Revision 1

As-bearing new mineral species from Valletta mine, Maira Valley, Piedmont, Italy: II. Braccoite, $\text{NaMn}^{2+}_5[\text{Si}_5\text{AsO}_{17}(\text{OH})](\text{OH})$, description and crystal structure

FERNANDO CÁMARA^{1,2*}, ERICA BITTARELLO^{1,2}, MARCO E. CIRIOTTI³, FABRIZIO NESTOLA⁴,
FRANCESCO RADICA⁵ AND MARCO MARCHESINI⁶

¹Dipartimento di Scienze della Terra, Università degli Studi di Torino, via Tommaso
Valperga Caluso 35, I-10125 Torino, Italy

²CrisDi, Interdepartmental Centre for the Research and Development of Crystallography, via
Pietro Giuria 7, I-10125, Torino, Italy

³Associazione Micromineralogica Italiana, via San Pietro 55, I-10073 Devesi-Cirié, Torino,
Italy

⁴Dipartimento di Geoscienze, Università degli Studi di Padova, via Giovanni Gradenigo 6, I-
35131 Padova, Italy

⁵Dipartimento di Scienze Geologiche, Università degli Studi Roma Tre, largo San Leonardo
Murialdo 1, I-00146 Roma, Italy

⁶EEEP house, UNIR, Basing View, Basingstoke, Hampshire, RG21 4YY, United Kingdom

*correspondent author's e-mail: fernando.camaraartigas@unito.it

25 **ABSTRACT**

26 The new mineral species braccoite, ideally $\text{NaMn}^{2+}_5[\text{Si}_5\text{AsO}_{17}(\text{OH})](\text{OH})$, has been
27 discovered in the Valletta mine dumps, in Maira Valley, Cuneo province, Piedmont, Italy. Its
28 origin is probably related to the reaction between ore minerals and hydrothermal fluids. It
29 occurs as subhedral crystals that occurs in brown-red coloured thin masses, with pale yellow
30 streak and vitreous to resinous luster. Braccoite is associated with tiragalloite, of which new
31 data is provided, as well as gamagarite, hematite, manganberzeliite, palenzonaite, quartz,
32 saneroite, tokyoite, unidentified Mn oxides, organic compounds, and Mn arsenates and
33 silicates under study.

34 Braccoite is biaxial positive with refractive indices α 1.749(1), β 1.750(1), γ 1.760(1). It
35 is triclinic, space group $P\bar{4}$, with $a = 9.7354(4)$, $b = 9.9572(3)$, $c = 9.0657(3)$ Å, $\alpha = 92.691(2)^\circ$,
36 $\beta = 117.057(4)^\circ$, $\gamma = 105.323(3)^\circ$, $V = 740.37(4)$ Å³ and Z 2. Its calculated density is 3.56
37 g/cm³. The ten strongest diffraction lines of the observed X-ray powder diffraction pattern are
38 [d in Å, (I), (hkl): 3.055 (69)(221), 3.042 (43)(102), 3.012 (65)(324), 2.985 (55)(234), 2.825
39 (100)(213), 2.708 (92)(220), 2.627 (43)(232), 2.381 (58)(444), 2.226 (25)(214), and 1.680
40 (433)(36). Chemical analyses by WDS electron microprobe gave (wt%): Na₂O 4.06, CaO
41 0.05, MnO 41.76, MgO 0.96, Al₂O₃ 0.04, CuO 0.02, SiO₂ 39.73, As₂O₅ 6.87, V₂O₅ 1.43, SO₃
42 0.01, and F 0.04. H₂O 2.20 was calculated on the basis of 2OH groups p.f.u. Raman
43 spectroscopy confirmed the presence of (SiO₄)⁴⁻, (AsO₄)³⁻ and OH groups. The empirical
44 formula calculated on the basis of Σ cations-(Na,K) = 11 p.f.u., in agreement to the results of
45 crystal structure, is $\text{Na}_{1.06}(\text{Mn}^{2+}_{4.46}\text{Mn}^{3+}_{0.32}\text{Mg}_{0.19}\text{V}^{3+}_{0.01}\text{Al}_{0.01}\text{Ca}_{0.01})[\text{Si}_5(\text{As}_{0.48}\text{Si}_{0.37}\text{V}^{5+}_{0.15})\text{O}_{17}$
46 $(\text{OH})](\text{OH}_{0.98}\text{F}_{0.02})$, the simplified formula is $\text{Na}(\text{Mn},\text{Mg},\text{Al},\text{Ca})_5[\text{Si}_5(\text{As}, \text{V},$
47 $\text{Si})\text{O}_{17}(\text{OH})](\text{OH},\text{F})$.

48 Single crystal X-ray diffraction allowed us to solve the structure by direct methods and
49 revealed that braccoite is the As-dominant analogue of saneroite. The structure model was
50 refined on the basis of 4389 observed reflections to R_1 3.47 %. Braccoite is named in honor of
51 Dr. Roberto Bracco (b. 1959), a systematic collector with a special interest in manganese
52 minerals. The new mineral was approved by IMA 2013-093.

53
54 **Keywords:** braccoite, saneroite, arseno-silicates, tiragalloite, new mineral species, crystal
55 structure, Raman, Valletta, Piedmont, Italy

57

INTRODUCTION

58 This is the second of a series of new mineral descriptions of As-bearing minerals from
59 Valletta mine (Cámara *et al.* 2014). The sample containing braccoite, the As-analogue of
60 saneroite, was collected by one of the authors (MM) in 2012 in the dumps of Valletta mine,
61 Vallone della Valletta, Canosio municipality, Maira Valley, Cuneo province, Piedmont, Italy
62 (44°23'54" N, 7°5'42" E, 2536 m asl).

63 The name is in honour of Dr. Roberto Bracco (b. 1959), a systematic collector with a
64 special interest in manganese minerals (Barresi *et al.*, 2005; Bracco and Balestra, 2014). He
65 has authored or coauthored several publications on systematic mineralogy, especially devoted
66 to new occurrences in Liguria (Bracco *et al.*, 2006; 2012).

67 A fragment of the holotype material is deposited in the mineralogical collections of the
68 Museo Regionale di Scienze Naturali di Torino, Sezione di Mineralogia, Petrografia e
69 Geologia, Torino, Italy, catalogue number M/15939.

70 Braccoite is intergrown with tiragalloite, which is an infrequent mineral. For this reason
71 we provide additionally chemical and Raman spectrum of tiragalloite [$\text{Mn}^{2+}_4\text{As}^{5+}\text{Si}_3\text{O}_{12}(\text{OH})$]
72 from Valletta mine.

73

74 GEOLOGICAL SETTING AND MINERAL OCCURRENCE

75 Geological and historical brief information is provided in Cámara *et al.* (2014). The
76 deposit at Valletta mine has never been studied from a genetic point of view and available
77 geological data for the area are of limited detail. Other than the historic texts, there is no
78 mention in the literature of the occurrence of metalliferous mineralization in this locality.
79 Preliminary work carried out during sampling showed that it is a small iron deposit with
80 subordinate manganese, in quartzites with quartz veins that contain a large variety of mineral
81 phases rich in arsenic, vanadium, barium and strontium. The volume of mineralized body is
82 however rather limited in surface.

83 The rock hosting braccoite is compact, granular, dark red verging on black quartzite.
84 Blocks of this material have been dug and piled up in a small landfill where they are mixed
85 with calcareous rocks also from the excavated material.

86 Braccoite is strictly associated with tiragalloite, and with gamagarite, hematite,
87 manganberzeliite, palenzonaite, quartz, saneroite, tokyoite, unidentified Mn oxides, organic
88 compounds, and Mn arsenates and silicates under study. These findings make in terms of
89 mineralogical variety the small dump of the old Valletta mine one of the richest Italian
90 deposits of arsenates and silicoarsenates mineral phases, like those of Val Graveglia (Antofilli

91 *et al.* 1983; Borgo and Palenzona, 1988; Palenzona, 1991, 1996; Marchesini and Pagano,
92 2001). Other As-rich minerals found in the rock samples collected in the dump, although not
93 strictly associated with braccoite are: adelite $\text{CaMg}(\text{AsO}_4)(\text{OH})$, arsenioleite-caryinite series
94 $(\text{Ca,Na})\text{NaMn}^{2+}(\text{Mn}^{2+},\text{Mg,Fe}^{2+})_2(\text{AsO}_4)_3$ - $(\text{Na,Pb})(\text{Ca,Na})\text{CaMn}^{2+}_2(\text{AsO}_4)_3$,
95 bariopharmacosiderite $\text{Ba}_{0.5}\text{Al}_4(\text{AsO}_4)_3(\text{OH})_4 \cdot 4\text{H}_2\text{O}$, berzeliite $\text{NaCa}_2\text{Mg}_2(\text{AsO}_4)_3$, grandaite
96 $\text{Sr}_2\text{Al}(\text{AsO}_4)_2(\text{OH})$ (IMA2013-059), and tilasite $\text{CaMg}(\text{AsO}_4)\text{F}$; these are found along with
97 aegirine, albite, azurite, baryte, braunite, calcite, diopside, fluorapatite, ganophyllite, gypsum,
98 ilmenite, hollandite, malachite, magnesio-arfvedsonite, magnesio-riebeckite, magnetite,
99 mimetite, muscovite, neotocite, opal, orthoclase, phlogopite, ranciéite, richterite, rutile,
100 rhodonite, talc, tetrahedrite, titanite and some other unknown phases under investigation.

101

102 **MINERALOGICAL CHARACTERIZATION**

103

104 **Appearance and physical properties**

105 Braccoite occurs as subhedral equant crystals, few hundred of micrometers accros,
106 with uneven fracture, grouped in thin masses, a few centimeters in size (Fig. 1), on granular
107 red-brown quartzite with reddish-brownish-black K-feldspar and compact quartz. In rare cases
108 the mineral forms rims around the remnants of protolithic quartz clasts. Individual crystals are
109 brown-red coloured and translucent. Braccoite has a pale yellow streak, a vitreous to resinous
110 luster, and does not fluoresce under SW or LW ultraviolet light. Braccoite is optically biaxial
111 positive, with a $2V_{\text{meas}} = 26(2)^\circ$ and $2V_{\text{calc}} = 35^\circ$. The measured refractive indices are $\alpha =$
112 $1.749(1)$, $\beta = 1.750(1)$, and $\gamma = 1.760(1)$ (589 nm). Braccoite is weakly pleochroic with X =
113 brownish yellow, Y = dark yellow, Z = yellow. The mineral is brittle and no cleavage and
114 parting are observed. Hardness and density were not measured due to the small crystal size
115 and because it occurs intimately intergrown with tiragalloite. The calculated density obtained
116 from the empirical formula and unit-cell parameters of the single crystal used for the crystal-
117 structure determination is 3.56 g/cm^3 .

118

119 **Chemical data**

120 Chemical composition of braccoite was determined using a Cameca SX-50 electron
121 microprobe (WDS mode) at the Department of Geosciences (Università di Padova) on a thin
122 section obtained from the holotype close to the place where the crystal used for the diffraction
123 study was extracted. Major and minor elements were determined at 20 kV accelerating
124 voltage and 20 nA beam current (beam size $2 \mu\text{m}$), with 40 to 20 s counting time on both peak

125 and background. X-ray counts were converted to oxide wt% using the PAP correction
126 program supplied by Cameca (Pouchou and Pichoir, 1984; 1985). The crystals studied in the
127 thin section (Fig. 2) were found to be homogeneous. Fe, Sb and Pb were analysed for but
128 were below detection limits. H₂O was calculated on the basis of 2OH groups p.f.u.
129 (Nagashima and Armbruster, 2010a). The average of 5 analyses are given in Table 1a. Low
130 totals are related to the difficulty of preparing good thin sections of polymineralic aggregates,
131 but have been also reported for saneroite samples (Nagashima and Armbruster, 2010a).

132 The empirical formula, calculated on the basis of 19 O a.p.f.u. and considering 2(OH)
133 is, within rounding errors, Na_{1.06}(Mn²⁺_{4.46}Mn³⁺_{0.32}Mg_{0.19}Al_{0.01}Ca_{0.01})_{Σ4.99} [(Si_{5.36}As_{0.48}V_{0.15})_{Σ5.99}
134 O₁₇(OH)] (OH_{0.98}F_{0.02}). Alternatively, the empirical formula, calculated on the basis of Σ
135 cations-(Na,K) = 11, Mn²⁺/Mn³⁺ ratio calculated in order to obtain [2(OH)-(Na-0.5)] groups
136 p.f.u. [Mn³⁺/(total Mn) = 0.066] and tetrahedral V⁵⁺ calculated as 6 – (Si + As), and excess V
137 is assigned to the octahedral sites as V³⁺, following Nagashima and Armbruster (2010a),
138 within rounding errors, is Na_{1.06}(Mn²⁺_{4.46}Mn³⁺_{0.32}Mg_{0.19}V³⁺_{0.01}Al_{0.01}Ca_{0.01})_{Σ=5.00}
139 [Si_{5.37}As⁵⁺_{0.48}V⁵⁺_{0.15}O₁₇(OH)] (OH_{0.98}F_{0.01}). The simplified formula can be written as:
140 NaMn²⁺₅[Si₅AsO₁₇(OH)](OH), which requires Na₂O 3.78, MnO 43.31, SiO₂ 36.68, As₂O₅
141 14.03, and H₂O 2.20, total 100 wt%. The presence of OH was confirmed by micro-Raman
142 spectroscopy. The mean refractive index *n* of braccoite, the calculated density and the
143 empirical formula yielded a Gladstone-Dale compatibility index (Mandarino 1979, 1981) of
144 0.020 rated as excellent. Braccoite is unreactive and insoluble in 2 M and 10% HCl, and 65%
145 HNO₃.

146 In Table 1b we show the comparison between the chemical data of tiragalloite
147 [Mn²⁺₄As⁵⁺Si₃O₁₂(OH)] from Valletta mine and tiragalloite from type-locality of Molinello
148 mine (Ne, Val Graveglia, Liguria, Italy) reported by Gramaccioli *et al.* (1980). Considering a
149 stoichiometric H₂O content in order to have one (OH) group per formula unit (p.f.u.), i.e. 1.46
150 wt % of H₂O, and 13 oxygen atoms p.f.u., the formula corresponding to the average of 3
151 analyses is (Mn²⁺_{3.92}Mg_{0.06}Na_{0.03})_{Σ4.01}(As⁵⁺_{0.87}V⁵⁺_{0.05}Si⁴⁺_{0.09})_{Σ1.01}Si₃O₁₂(OH_{0.96}F_{0.04}).

152

153 **Micro-Raman spectroscopy**

154 The Raman spectrum of braccoite (Fig. 3) was obtained at the Dipartimento di Scienze
155 della Terra (Università di Torino) using a micro/macro Jobin Yvon LabRam HRVIS,
156 equipped with a motorized x-y stage and an Olympus microscope. The backscattered Raman
157 signal was collected with 50× objective and the spectrum was obtained for a non-oriented
158 crystal. The 632.8 nm line of an He-Ne laser was used as excitation; laser power (20 mW)

159 was controlled by means of a series of density filters. The minimum lateral and depth
160 resolution was set to a few μm . The 532 nm line of a Nd laser was also used as excitation;
161 laser power (80 kW) was dosed by means of a series of density filters. An aperture of 200 μm
162 was used to reduce the beam dose. The lateral and depth resolution were about 2 and 5 μm ,
163 respectively. The system was calibrated using the 520.6 cm^{-1} Raman band of silicon before
164 each experimental session. Spectra were collected with multiple acquisitions (2 to 6) with
165 single counting times ranging between 20 and 180 s. The spectrum was recorded using the
166 LabSpec 5 program from 200 to 4000 cm^{-1} . Spectra collected with both lasers were
167 equivalent. Spectrum reported in Fig. 3 was collected with the 632.8 nm line of the He-Ne
168 laser.

169 There is a close match between the braccoite spectrum and that of saneroite from type
170 locality of Molinello mine (Graveglia Valley, Liguria, Italy) in the database RRUFF
171 (R060488) (Downs, 2006). All bands observed between 700 and 1000 cm^{-1} are characteristic
172 of the two groups present in braccoite, SiO_4^{4-} and $\text{AsO}_3(\text{OH})^{2-}$ (Myneni *et al.*, 1998a,b;
173 Nakamoto, 1986). The spectrum shows intense bands around 829, 907 and 932 (respect to
174 823, 909 and 936 cm^{-1} for saneroite R060488 at RRUFF) and weak peaks at 706 and 748 cm^{-1}
175 (700 and 729 cm^{-1} for saneroite R060488 at RRUFF). The intense peak at 1017 cm^{-1} with a
176 weak shoulder at 1040 cm^{-1} may be assigned to the ν_1 symmetric stretching mode of the SiO_4
177 units (Mills *et al.*, 2005) (1011 and 1022 cm^{-1} for saneroite R060488) while the region
178 assigned in the pyroxenes to the stretching modes of the Si-O bonds is present in the braccoite
179 spectrum at 665 cm^{-1} (respect to 660 cm^{-1} for saneroite R060488). Bending modes of O-Si-O
180 are observed at 525 cm^{-1} and 563 cm^{-1} for braccoite, while Raman spectrum of saneroite
181 R060488 shows a single weak band around 523 cm^{-1} . Cation-oxygen vibration modes appear
182 in the low region of the spectrum below 460 cm^{-1} : weak and broad peaks are observed at 226,
183 261, 291, 360, 390 and 451 cm^{-1} (respect to 228, 281, 343, 376, 436 cm^{-1} for saneroite
184 R060488). The Raman spectrum of braccoite shows a broad envelope of overlapping bands
185 centered upon 3361 and 3507 cm^{-1} , which are characteristic of OH stretching modes, in
186 accordance with the presence of hydroxyl groups in the structure (spectrum of saneroite
187 R060488 was collected only for $< 1200 \text{ cm}^{-1}$).

188 Tiragalloite is intergrown with braccoite in rocks from Valletta mine. There is no
189 available Raman spectrum for tiragalloite and therefore we collected spectra also for this
190 mineral phase (Fig. 4). The spectrum shows a strong absorption centered at 869 cm^{-1} with
191 three shoulders at 803, 836 and 902 cm^{-1} , two intense peaks at 661 and 647 cm^{-1} and weaker
192 peaks at 960, 975 cm^{-1} and a broad band at $\sim 1004 \text{ cm}^{-1}$. As for braccoite and saneroite, the

193 frequency separations between the bands due to the asymmetric and the symmetric stretches
194 of the anionic groups $(\text{SiO}_4)^{4-}$ and $(\text{AsO}_4)^{3-}$, present tiragalloite vary strongly from one
195 structure to another, and cannot be assigned with conviction (Hawthorne *et al.*, 2013). Bands
196 with frequencies between 250 and 600 cm^{-1} correspond to $(\text{SiO}_4)^{4-}$ and $(\text{AsO}_4)^{3-}$ vibrations
197 (286, 320, 364, 398, 481, 508 and 549 cm^{-1}), while weak and broad bands lower than 250 cm^{-1}
198 correspond to lattice modes (153, 181 and 218 cm^{-1}). In the region between 1200 and 3000
199 cm^{-1} the spectrum displays a considerable amount of noise (a broad envelope of overlapping
200 bands centered upon 1635, 1702 and 1799 cm^{-1}) and this is a result of the low intensity of the
201 bands. In accordance with the presence of hydroxyl groups in the structure a wide and weak
202 band at $\sim 3100 \text{ cm}^{-1}$. Based on the Libowitzky (1999) correlation, the band at $\sim 3100 \text{ cm}^{-1}$ can
203 be possibly assigned to the O11–H11...O1 bond present in tiragalloite (O11...O1 = 2.725 Å
204 corresponding to 3257 cm^{-1} , using crystal data provided by Nagashima and Armbruster
205 2010b).

206

207 **X-ray diffraction**

208 The powder X-ray diffraction pattern of braccoite was obtained at CrisDi
209 (Interdepartmental Centre for the Research and Development of Crystallography, Torino, Italy)
210 using an Oxford Gemini R Ultra diffractometer equipped with a CCD area detector, with
211 graphite-monochromatized $\text{MoK}\alpha$ radiation. Indexing of the reflections was based on a
212 calculated powder pattern obtained from the structural model, using the software LAZY
213 PULVERIX (Yvon *et al.*, 1977). Experimental and calculated data are reported in Table 2. The
214 unit-cell parameters refined from the powder data with the software GSAS (Larson and Von
215 Dreele, 1994) are $a = 9.756(6)$, $b = 9.961(7)$, $c = 9.087(7)$ Å, $\alpha = 92.23(5)^\circ$, $\beta = 117.27(5)^\circ$, γ
216 $= 105.21(4)^\circ$, $V = 742.2(9)$ Å³.

217 Single-crystal X-ray diffraction data were collected using an Oxford Gemini R Ultra
218 diffractometer equipped with a CCD area detector at CrisDi with graphite-monochromatized
219 $\text{MoK}\alpha$ radiation ($\lambda = 0.71073$ Å). A crystal fragment showing sharp optical extinction
220 behaviour was used for collecting intensity data. No crystal twinning was observed. Crystal
221 data and experimental details are reported in Table 3. The intensities of 7946 reflections with
222 $-13 < h < 14$, $-14 < k < 14$, $-13 < l < 13$ were collected to $64.4^\circ 2\theta$ using 1° frame and an
223 integration time of 20 s. Data were integrated and corrected for Lorentz and polarization
224 background effects, using the package CrysAlisPro, Agilent Technologies, Version
225 1.171.36.20 (release 27-06-2012 CrysAlis171.36.24). Data were corrected for empirical
226 absorption using spherical harmonics, implemented in the SCALE3 ABSPACK scaling

227 algorithm. Refinement of the unit-cell parameters was based on 4389 measured reflections
228 with $I > 10\sigma(I)$. At room temperature, the unit-cell parameters are a 9.7354(4), b 9.9572(3), c
229 9.0657(3) Å, α 92.691(2)°, β 117.057(4)°, γ 105.323(3)°, V 740.37(4) Å³, space group $P\bar{1}$
230 and Z 2. The $a:b:c$ ratio is 0.978:1:0.910. A total of 4911 independent reflections were
231 collected and the structure was solved and refined using the SHELX set of programs
232 (Sheldrick, 2008).

233

234 DESCRIPTION OF THE STRUCTURE

235 Structure model

236 The crystal structure of braccoite (Figure 5) is topologically identical to that of the
237 hydropyroxenoid saneroite: a single isolated chain of SiO₄ tetrahedra with a five repeat plus
238 an appendix of a sixth tetrahedron where Si_{1-x}As_x substitution occurs (Si_{1-x}V⁵⁺_x in saneroite).
239 which repeats laterally by a centre of symmetry forming a layer of tetrahedra parallel (1+1).
240 Five octahedral sites occupied by Mn (mostly Mn²⁺, with some Mn³⁺) form a band which runs
241 parallel to two single chains of tetrahedra attached up and down. Laterally the bands are
242 separated by channels occupied partially by two independent Na sites, one completely
243 occupied and another with partial occupation. The structure of braccoite was therefore refined
244 starting from the atom coordinates of saneroite excluding H sites (Nagashima and Armbruster,
245 2010a). Nomenclature of sites follows therefore those of the aforementioned authors.
246 Scattering curves for neutral and ionized atoms were taken from International Tables for
247 Crystallography (Wilson, 1992). Site-scattering values were refined for the cation sites using
248 two scattering curves contributing proportionally and constrained sum to full occupancy:
249 Mn²⁺ and Mg were used for the sites $Mn(1-5)$; Si⁴⁺ full occupancy was fixed at the $T(1-5)$
250 sites, while Si⁴⁺ and As were used at $T(6)$ site; Na⁺ was used for the $Na(1)$ and $Na(2)$ sites,
251 although the occupancy was held fixed at $Na(1)$ and refined at $Na(2)$. After converging, the
252 positions of two H atoms [$H(7)$ and $H(19)$ sites] were located in difference Fourier maps and
253 added to the model; atom coordinates of H sites were refined and isotropic thermal parameters
254 were constrained to be 1.2 times the isotropic equivalent of the oxygen atom of the hydroxyl
255 group assuming a riding motion model, while a soft constraint of 0.98 Å (Franks, 1973) was
256 applied to the $H(19)$ –O(19) distance. Structure refinement converged to $R_1 = 0.0347$ for 4389
257 reflections with $F_o > 4\sigma(F_o)$ and 0.0413 for all 4911 data. Tables 4, 5 and 6 report atomic
258 coordinates, the displacement parameters and selected bond distances and angles respectively
259 for braccoite. Bond valence calculations using the parameters of Brown (1981) are reported in
260 Table 7. (CIF¹ and structure factor list files are available on deposit).

261

262 **Site occupancies**

263 *Cation sites*

264 There are 13 cation sites in the braccoite structure: 6 sites are 4-coordinated, 5 sites are
265 6-coordinated, and 2 are 8-coordinated. One out of the six 4-coordinated sites, the *T*(6) site,
266 has a higher mean atomic number [24.17(6) electrons per site (e.p.s.) versus 14 e.p.s. for the
267 other 5 sites, Table 4], and $\langle T-O \rangle$ is larger than that the other 5 sites (1.675 Å vs. a mean of
268 1.624 Å for the other 5 sites, Table 6). Chemical analyses report the presence of both V^{5+} and
269 As^{5+} that can order in a site with tetrahedral coordination. The refined site scattering is > 23
270 e.p.s. and therefore implies dominance of As in presence of sufficient amount of Si. The latter
271 is confirmed by EMP analyses (Table 1a). In presence of concomitant Si-V-As solid solution
272 in a cation site with tetrahedral coordination, the size of the tetrahedron is not sufficient to
273 provide the actual dominance of As^{5+} versus V^{5+} because they have very similar ionic radii
274 (0.335 and 0.355 Å, respectively, Shannon 1976). While distances observed in the studied
275 crystal (Table 6) are compatible with a Si–V substitution (values of 1.68–1.69 Å are usually
276 found for saneroite, Nagashima and Armbruster, 2010a, and ca. 1.70 Å for medaite,
277 Nagashima and Armbruster, 2010b), It is worth noting that besides the chemical strain due to
278 a three component solid solution, the *T*(6) is not the most distorted 4-coordinated site in the
279 structure: the *T*(5) shows the highest angle variance [σ^2 41.72, computed according to
280 Robinson *et al.* 1971, Table 6] as similarly observed in saneroite ($\sigma^2 = 40.00$, Basso and Della
281 Giusta, 1980).

282 Regarding the 5 sites 6-coordinated, all are Mn^{2+} dominant. However, site *Mn*(3) is
283 significantly smaller (2.183 Å versus 2.20–2.25 Å, Table 6). This can be interpreted as
284 ordering of a lighter and smaller Mg cation, which is present in the chemical analyses. Yet
285 ordering all the Mg at the *Mn*(3) site would require a site scattering value lighter than that
286 observed. On the other hand, a small quantity of Mn^{3+} has been inferred in the chemical
287 formula (see Chemical data section) in order to achieve charge balance assuming full
288 occupancy of H at the *H*(7) and *H*(19) sites. In addition, Nagashima and Armbruster (2010a)
289 confirmed the presence of a limited quantity of Mn^{3+} in saneroite from Molinello (Val
290 Graveglia, Italy) by using the ratio of the X-ray intensities of the *MnL* β and *MnL* α lines after
291 the method of Albee and Chodos (1970) and Kimura and Akasaka (1999). Therefore, we
292 assumed also for braccoite a limited amount of Mn^{3+} (0.066 Mn^{3+}/Mn_{total}). Incidentally, other
293 Mn^{3+} phases have been found at the Valletta mine (es. grandaite, Cámara *et al.*, 2014) and all
294 the iron-bearing phases have just Fe^{3+} . Because there is not a high bond valence contribution

295 to the *Mn*(3) site (Table 7) it is probable that Mn^{3+} distributes also in the other two smaller
296 sites, *Mn*(2) and *Mn*(4). In the structure of braccoite there is also one octahedron that is
297 slightly larger than the others, the *Mn*(1) site. Apparently, it should host the very small
298 amount of Ca in the analyses, although that amount is not enough to justify the observed size
299 enlargement. However, Ca could also distribute at the *Na*(1) or *Na*(2) sites. The *Mn*(1) site is
300 also the more distorted ($\sigma^2 = 170.51$, compared to values ranging between 55.18 and 86.77,
301 Table 6). This is possibly due to the fact that the oxygen at O(16) acts as bond donor to the
302 proton at *H*(19) and that it is the only octahedron that shares an edge with a tetrahedron, the
303 *T*(5) site, which is also the most distorted tetrahedron. The O(5)-O(14) edge involves two
304 anion sites with among the highest and the lowest bond valence contribution, respectively
305 (Table 7) and is also the shortest. Hence there is a possible charge-shielding mechanism
306 operated by the electronic clouds of both oxygen atoms.

307 The 8-coordinated sites host Na atoms. The *Na*(1) site has full occupancy and bond
308 distances compatible with 1 a.p.f.u. of Na (Table 8), while the *Na*(2) site shows a refined site
309 scattering which indicates approx. half occupancy of Na (Table 4). This site shares four edges
310 with four Si tetrahedra and two edges with two Mn octahedra [*Mn*(2) and *Mn*(5)]. This is
311 probably impeding the full occupancy of this site and produces a rather distorted bonding
312 environment.

313 Taking into consideration the observed site scattering values and those obtained from
314 EMP analyses, the agreement for all cations sites is within 2% relative error, with slightly
315 lighter values from diffraction data than obtained from chemical analyses (230.8 electrons per
316 formula unit, e.p.f.u., versus 233.9 e.p.f.u., respectively). Site-distribution according to the
317 structure refinement (site scattering and bond distances) and electron microprobe data results
318 give full occupancy of Si at the *T*(1-5) sites, *T6* ($As^{5+}_{0.48}Si_{0.37}V^{5+}_{0.15}$), *Mn*1
319 ($Mn^{2+}_{0.98}Mg_{0.01}Ca_{0.01}$), *Mn*2 ($Mn^{2+}_{0.87}Mn^{3+}_{0.07}Mg_{0.06}$), *Mn*3
320 ($Mn^{2+}_{0.66}Mn^{3+}_{0.22}V^{3+}_{0.01}Al_{0.01}Mg_{0.10}$), *Mn*4 ($Mn^{2+}_{0.96}Mn^{3+}_{0.03}Mg_{0.01}$), *Mn*5 ($Mn^{2+}_{0.99}Mg_{0.01}$),
321 *Na*1 ($Na_{1.00}$), *Na*2 ($Na_{0.56}$), with an overall positive charge of 36.53. Table 8 reports the
322 agreement between observed values and those calculated from chemical composition after site
323 assignment.

324

325 *Anion sites*

326 There are 19 anion sites in the structure of braccoite, 10 are 3-coordinated and the rest
327 are 4-coordinated (Table 7). There are three anion sites with a bond valence incidence
328 significantly higher than 2 v.u.: O(4), O(5) and O(6). The same atoms show also high bond

329 valence incidence for saneroite (Basso and Della Giusta, 1980; Nagashima and Armbruster
330 2010a), in particular O(4), which is 3-coordinated; at the O(4) site, the contribution from $T(3)$
331 and $T(4)$ is already 2.011 v.u. and therefore the contribution from the $Na(2)$ site (0.134 v.u.,
332 Table 7) oversaturates this anion site. This is in fact a strong another restriction for a full
333 occupancy of the $Na(2)$ site (see above).

334 Two anion sites are actually 3-coordinated [O(11) and O(16)] but act as donor of two
335 respective hydrogen bonds at O(7) and O(19). Chemical analyses show a very limited amount
336 of fluorine. While it is not possible to assess in which site the fluorine orders, it is highly
337 probable that it orders at the O(19) site: this site receives a bond valence contribution of 1.091
338 v.u. (Table 7) and therefore hosts an (OH) group, which belongs to three octahedra of two
339 $Mn(3)$ and one $Mn(2)$ site. The Raman spectrum at Figure 3 shows a broad envelope of
340 overlapping bands centered upon 3361 and 3507 cm^{-1} , which are reflecting the two essential
341 next neighbor configurations: $Mn^{2+}Mn^{2+}Mn^{2+}$ and $Mn^{3+}Mn^{3+}Mn^{2+}$, while other configurations
342 are also possible, i.e. $MgMgMn^{2+}$, $Mn^{3+}Mn^{3+}Mn^{3+}$ or even $MgMgMg$, yielding in the overall
343 a broad band. Hydrogen bonding is also present at the O(7) anion site. However, in this case,
344 a short distance with another oxygen atom at the O(11) anion site (2.48 Å) along with a
345 similar bond valence contribution, of 1.531 for O(7) and 1.524 v.u. for O(11), is probably
346 responsible for a very strong hydrogen bond (see later).

347

348 **Hydrogen bonding**

349 Strong hydrogen bonding is present in the braccoite structure as it was observed in
350 saneroite. A close inspection of Table 7 shows that there are four oxygen sites with bond
351 valence incidence < 1.8 v.u.: O(7), O(11), O(16) and O(19). There is one very short acceptor-
352 donor distance corresponding to a very strong hydrogen bond [O(7)...O(11) = 2.48 Å, Table
353 6], and another longer distance corresponding to a medium strength hydrogen bond
354 (O(19)...O(16) = 2.855 Å, Table 6). Using the relation $\nu(\text{cm}^{-1}) =$
355 $3592 - 304 \times 10^9 \cdot \exp(-d(\text{O} \dots \text{O})/0.1321)$ (Libowitzky, 1999), we should expect bands at 1456
356 and 3467 cm^{-1} . While frequencies at ca. 3500 cm^{-1} are observed in the Raman spectrum of
357 braccoite (Fig. 3) the expected band around 1400 cm^{-1} is not visible in the spectrum. The
358 positions of two hydrogen atoms were observed in the Fourier-difference maps at
359 convergence and were added to the model. In particular, the position observed for the $H(7)$
360 atom shows a bond with oxygen at the O(7) anion site with a short $H(7) \dots O(11)$ distance of
361 1.62(4) Å. The position of the corresponding hydrogen atom in saneroite was not detected by
362 Basso and Della Giusta (1980) but was found with very similar atom coordinates by

363 Nagashima and Armbruster (2010a) ($x = 0.937(5)$ $y = 0.493(4)$ $z = 0.820(5)$) for braccoite and
364 $x = 0.940(3)$ $y = 0.506(3)$ $z = 0.815(4)$) for saneroite specimen 1 of Nagashima and
365 Armbruster, 2010a, Table 3), and in fact a band at ca. 1400 cm^{-1} was observed in the FT-IR
366 spectrum collected on saneroite from Molinello by Brugger *et al.* (2006). The fact that both
367 O(7) and O(11) show an equivalent bond valence contribution (Table 7), suggests a plausible
368 disordered environment for this proton. Such a situation, with a disordered position for H, has
369 been already observed in another related pyroxenoid structure, serandite
370 ($\text{NaMn}_2[\text{Si}_3\text{O}_8(\text{OH})]$), which shows a O...O distance of 2.464–2.468 Å (Jacobsen *et al.*, 2000)
371 and for which the IR O–H stretching mode was found at 1386 cm^{-1} (Hammer *et al.*, 1998).
372 Another topologically related structure is scheuchzerite ($\text{NaMn}^{2+}_9[\text{Si}_9\text{V}^{5+}\text{O}_{28}(\text{OH})](\text{OH})_3$;
373 Brugger *et al.*, 2006), which has also a very strong hydrogen bond among O(26) and O(29)
374 anion sites, distant by 2.35 Å (Brugger *et al.*, 2006). In this case a band is observed at 1466 cm^{-1}
375 in the FTIR spectrum, which can correspond to the strong hydrogen bond. It should be
376 also taken into account that the H(7) site is at a distance of 2.09(5) Å of the Na(2) site, which
377 is not far of the Na–H distance in NaH (1.913 Å; Chen *et al.*, 2005) and this surely stresses the
378 bonding environment of the proton at ca. half of the H(7) sites.

379

380 RELATED MINERALS

381 Braccoite, $\text{NaMn}^{2+}_5[\text{Si}_5\text{AsO}_{17}(\text{OH})](\text{OH})$, is the As–dominant analogue of saneroite,
382 $\text{NaMn}^{2+}_5[\text{Si}_5\text{V}^{5+}\text{O}_{17}(\text{OH})](\text{OH})$ (Basso and Della Giusta, 1980; Lucchetti *et al.*, 1981;
383 Nagashima and Armbruster, 2010a). For the dominant cation in T6 site Nagashima and
384 Armbruster (2010) proposed to add a suffix, i.e. “saneroite-(V)”, “saneroite-(Si)” and
385 “saneroite-(As)”. In the recent IMA guidelines, Hatert *et al.* (2013) allow the use of any
386 another name confirming that “mineral names are chosen by the authors of new mineral
387 species, according to functional guidelines established by the Nickel & Grice (1998)”. A new
388 name was chosen to avoid suffixing saneroite so as to preserve *in toto* this “well-established
389 name” and also to meet with the preferences of the collectors community.

390 Braccoite has also structural similarity with scheuchzerite,
391 $\text{NaMn}^{2+}_9[\text{Si}_9\text{V}^{5+}\text{O}_{28}(\text{OH})](\text{OH})_3$ (Brugger *et al.*, 2006; Palenzona *et al.*, 2006; Roth, 2007):
392 while saneroite/braccoite have a silicate single-chain with five tetrahedra in the repeating unit
393 – with an additional tetrahedron branching sideways (Fig. 5) – scheuchzerite has a chain that
394 consists of the branched saneroite chain with additional attached silicate tetrahedra,
395 configuring “loops” (Brugger *et al.*, 2006). These “loops” are also present in a new Na–Mn
396 borosilicate, steedite $\text{NaMn}^{2+}_2[\text{Si}_3\text{BO}_9(\text{OH})](\text{OH})$ (IMA2013-052), which crystal structure

397 closely resembles those of the sérandite-pectolite pyroxenoids and it is also broadly similar to
398 the crystal structure of scheuchzerite (Haring and McDonald, 2014).

399 Braccoite is the first As member of the saneroite family and in Table 9 we have
400 reported a comparison of the properties of the members. In the Strunz System (Strunz and
401 Nickel, 2001) braccoite fits in subdivision 9.D.K, inosilicates with 5-periodic single chains.
402 Its equivalent synthetic compound is not known.

403

404 **ACKNOWLEDGMENTS**

405 The authors are indebted to Bruno Lombardo, who passed away some days after the
406 identification of this new species, for his assessment support in field work at the Valletta.
407 Mariko Nagashima, Gerald Giester, Peter Leverett and associate editor Stuart Mills are
408 thanked for their constructive comments on the manuscript. FC and EB thank MIUR and AMI
409 for the co-funding of a research contract for EB for the year 2013. Raul Carampin (CNR-IGG,
410 Padova, Italy) is thanked for his support on the WDS analysis.

411

412 **REFERENCES**

- 413 Albee, A. and Chodos, A.A. (1970) Semiquantitative electron microprobe determination of
414 $\text{Fe}^{2+}/\text{Fe}^{3+}$ and $\text{Mn}^{2+}/\text{Mn}^{3+}$ in oxides and silicates and its application to petrologic
415 problems. *American Mineralogist*, **55**, 491–501.
- 416 Albrecht, J. (1990) An As-rich manganiferous mineral assemblage from the Ködnitz Valley
417 (Eastern Alps, Austria): geology, mineralogy, genetic considerations, and implications for
418 metamorphic Mn deposits. *Neues Jahrbuch für Mineralogie, Monatshefte*, 363–375.
- 419 Antofilli, M., Borgo, E., and Palenzona, A. (1983) *I nostri minerali. Geologia e mineralogia*
420 *in Liguria*, 296 p. SAGEP Editrice, Genova (in Italian). Barresi, A.A., Kolitsch, U.,
421 Ciriotti, M.E., Ambrino, P., Bracco, R., and Bonacina, E. (2005) La miniera di
422 manganese di Varenche (Aosta, Italia nord-occidentale): ardenite, arseniopleite,
423 manganberzeliite, pirofanite, sarkinite, thortveitite, nuovo As–Sc–analogo della
424 metavariscite e altre specie. *Micro*, **3**, 81–122 (in Italian).
- 425 Basso, R., and Della Giusta, A. (1980) The crystal structure of a new manganese silicate.
426 *Neues Jahrbuch für Mineralogie, Abhandlungen*, **138**, 333–342.
- 427 Bracco, R. and Balestra, C. (2014) La miniera di Monte Nero, Rocchetta Vara, La Spezia,
428 Liguria: minerali classici e novità. *Micro*, **12**, 2–28 (in Italian).
-

- 429 Bracco, R., Balestra, C., Castellaro, F., Mills, S.J., Ma, C., Callegari, A.M., Boiocchi, M.,
430 Bersani, D., Cadoni, M., and Ciriotti, M.E. (2012) Nuovi minerali di Terre Rare da Costa
431 Balzi Rossi, Magliolo (SV), Liguria. *Micro*, **10**, 66–77 (in Italian).
- 432 Bracco, R., Callegari, A., Boiocchi, M., Balestra, C., Armellino, G., and Ciriotti, M.E. (2006)
433 Costa Balzi Rossi (Magliolo, Val Maremola, Savona, Liguria): una nuova località per
434 minerali di Terre Rare e scandio. *Micro*, **4**, 161–178 (in Italian).
- 435 Borgo, E. and Palenzona, A. (1988) *I nostri minerali. Geologia e mineralogia in Liguria.*
436 *Aggiornamento* 1988, 48 p. SAGEP Editrice, Genova (in Italian).
- 437 Brown, I.D. (1981) The bond-valence method: an empirical approach to chemical structure
438 and bonding. Pp. 1–30. *Structure and Bonding in Crystals II*, (M. O’Keeffe and A.
439 Navrotsky, editors), Academic Press, New York.
- 440 Brugger, J., Krivovichev, S., Meisser, N., Ansermet, S., and Armbruster, T. (2006)
441 Scheuchzerite, $\text{Na}(\text{Mn},\text{Mg})_9[\text{VSi}_9\text{O}_{28}(\text{OH})](\text{OH})_3$, a new single-chain silicate. *American*
442 *Mineralogist*, **91**, 937–943.
- 443 Cámara, F., Ciriotti, M.E., Bittarello, E., Nestola, F., Massimi, F., Radica, F., Costa, E.,
444 Benna, P., and Piccoli, G.C. (2014) As-bearing new mineral species from Valletta mine,
445 Maira Valley, Piedmont, Italy: I. Grandaite, $\text{Sr}_2\text{Al}(\text{AsO}_4)_2(\text{OH})$, description and crystal
446 structure. *Mineralogical Magazine*, (in press).
- 447 Chen Y.L., Huang, C.H. and Hu, W.P. (2005) Theoretical study of the small clusters of LiH,
448 NaH, BeH₂, and MgH₂. *The Journal of Physical Chemistry A*, **109**, 9627–9636.
- 449 Downs, R.T. (2006) The RRUFF Project: an integrated study of the chemistry,
450 crystallography, Raman and infrared spectroscopy of minerals. Program and Abstracts of
451 the 19th General Meeting of the International Mineralogical Association in Kobe, Japan.
452 O03-13
- 453 Franks, F., ed. (1973): *Water: a comprehensive treatise*, Vol. 2. Plenum, New York, 684 p.
- 454 Gramaccioli C. M., Griffin W.L., Mottana A. (1980) Tiragalloite, $\text{Mn}_4[\text{AsSi}_3\text{O}_{12}(\text{OH})]$, a new
455 mineral and the first example of arsenatotrisilicate. *American Mineralogist*, **65**, 947–952.
- 456 Hammer, V.M.F., Libowitzky, E., Rossman, G.R. (1998) Single crystal IR spectroscopy of
457 very strong hydrogen bonds in pectolite, $\text{NaCa}_2[\text{Si}_3\text{O}_8(\text{OH})]$, and serandite,
458 $\text{NaMn}_2[\text{Si}_3\text{O}_8(\text{OH})]$. *American Mineralogist*, **83**, 569–576.
- 459 Haring, M.M.M., McDonald A.M. (2014) Steedeite, $\text{NaMn}_2[\text{Si}_3\text{BO}_9](\text{OH})_2$: characterization,
460 crystal-structure determination, and origin. *Canadian Mineralogist*, **52**, 47-60.
-

- 461 Hatert, F., Mills, S.J., Pasero, M., Williams, P.A. (2013) CNMNC guidelines for the use of
462 suffixes and prefixes in mineral nomenclature, and for the preservation of historical
463 names. *European Journal of Mineralogy*, **25**, 113–115.
- 464 Hawthorne F.C., Abdu Y.A., Ball N.A., Pinch W.W. (2013) Carlfrancisite:
465 $\text{Mn}^{2+}_3(\text{Mn}^{2+}, \text{Mg}, \text{Fe}^{3+}, \text{Al})_{42}(\text{As}^{3+}\text{O}_3)_2(\text{As}^{5+}\text{O}_4)_4[(\text{Si}, \text{As}^{5+})\text{O}_4]_6[(\text{As}^{5+}, \text{Si})\text{O}_4]_2(\text{OH})_{42}$, a new
466 arseno-silicate mineral from the Kombat mine, Otavi Valley, Namibia. *American
467 Mineralogist*, **98**, 1693–1696.
- 468 Jacobsen, S.D., Smyth, J.R., Swope, R.J., Sheldon, R.I. (2000) Two proton positions in the
469 very strong hydrogen bond of serandite, $\text{NaMn}_2[\text{Si}_3\text{O}_8(\text{OH})]$. *American Mineralogist*, **85**,
470 745–752.
- 471 Kimura, Y. and Akasaka, M. (1999) Estimation of $\text{Fe}^{2+}/\text{Fe}^{3+}$ and $\text{Mn}^{2+}/\text{Mn}^{3+}$ ratios by electron
472 probe micro analyzer. *Journal of the Mineralogical Society of Japan*, **28**, 159–166 (in
473 Japanese with English abstract).
- 474 Larson, A.C., and Von Dreele, R.B. (1994) General Structure Analysis System (GSAS). Los
475 Alamos National Laboratory Report LAUR, 86–748.
- 476 Libowitzky, E. (1999) Correlation of OH stretching frequencies and O–H...O hydrogen bond
477 lengths in minerals. *Monatshefte für Chemie*, **130**, 1047–1059.
- 478 Lucchetti, G., Penco, A.M., and Rinaldi, R. (1981) Saneroite, a new natural hydrated Mn-
479 silicate. *Neues Jahrbuch für Mineralogie, Monatshefte*, 161–168. Mandarino, J.A. (1979)
480 The Gladstone-Dale relationship. Part III. Some general applications. *The Canadian
481 Mineralogist*, **17**, 71–76.
- 482 Mandarino, J.A. (1981) The Gladstone-Dale relationship. Part IV. The compatibility concept
483 and its application. *The Canadian Mineralogist*, **19**, 441–450.
- 484 Marchesini, M. and Pagano, R. (2001) The Val Graveglia Manganese District, Liguria, Italy.
485 *Mineralogical Record*, **32**, 349–379.
- 486 Mills, S.J., Frost, R.L., Klopogge, J.T., and Weier, M.L. (2005) Raman spectroscopy of the
487 mineral rhodonite. *Spectrochimica Acta*, **62**, 171–175.
- 488 Momma, K. and Izumi, F. (2011) "VESTA 3 for three-dimensional visualization of crystal,
489 volumetric and morphology data. *Journal of Applied Crystallography*, **44**, 1272–1276.
- 490 Myneni, S.C.B., Traina, S.J., Waychunas, G.A., and Logan, T.J. (1998a) Experimental and
491 theoretical vibrational spectroscopic evaluation of arsenate coordination in aqueous
492 solutions and solids. *Geochimica et Cosmochimica Acta*, **62**, 3285–3300.
-

- 493 Myneni, S.C.B., Traina, S.J., Waychunas, G.A., and Logan, T.J. (1998b) Vibrational
494 spectroscopy of functional group chemistry and arsenate coordination in ettringite.
495 *Geochimica et Cosmochimica Acta*, **62**, 3499–3514.
- 496 Nakamoto, K. (1986) Infrared and Raman Spectra of Inorganic and Coordination Compounds,
497 419 pp. Wiley, New York.
- 498 Nagashima, M., and Armbruster, T. (2010a) Saneroite: chemical and structural variations of
499 manganese pyroxenoids with hydrogen bonding in the silicate chain. *European Journal*
500 *of Mineralogy*, **22**, 393–402.
- 501 Nagashima, M., and Armbruster, T. (2010b) Ardennite, tiragalloite and medaite: structural
502 control of $(As^{5+}, V^{5+}, Si^{4+})O_4$ tetrahedra in silicates. *Mineralogical Magazine*, **74**, 55–71.
- 503 Palenzona, A. (1991) *I nostri minerali. Geologia e mineralogia in Liguria. Aggiornamento*
504 1990, p. 48. Amici Mineralogisti Fiorentini, Associazione Piemontese Mineralogia
505 Paleontologia & Mostra Torinese Minerali, Centro Mineralogico Varesino, Gruppo
506 Mineralogico “A. Negro” Coop Liguria (GE), Gruppo Mineralogico Lombardo, Gruppo
507 Mineralogico Paleontologico “3M” Ferraia (Savona), (in Italian).
- 508 Palenzona, A. (1996) *I nostri minerali. Geologia e mineralogia in Liguria, Aggiornamento*
509 1995. *Rivista Mineralogica Italiana*, **2**, 149–172 (in Italian).
- 510 Palenzona, A., Martinelli, A., Bracco, R., and Balestra, C. (2006) IMA 2004-044
511 (scheuchzerite) alla miniera di Gambatesa. *Prie*, **2**, 11–12 (in Italian)
- 512 Pouchou, J.L., and Pichoir, F. (1984) A new model for quantitative analysis: Part I.
513 Application to the analysis of homogeneous samples. *La Recherche Aérospatiale*, **3**,
514 13–38.
- 515 Pouchou, J.L., and Pichoir, F. (1985) ‘PAP’ $\phi(\rho Z)$ procedure for improved quantitative
516 microanalysis. In J.T. Armstrong, Ed., *Microbeam Analysis*, p. 104–106. San Francisco
517 Press, San Francisco, California.
- 518 Robinson, K., Gibbs, G.V., and Ribbe, P.H. (1971) Quadratic elongation: a quantitative
519 measure of distortion in coordination polyhedra. *Science*, **172**, 567–570.
- 520 Roth, P. (2007) Scheuchzerite. In *Minerals First Discovered in Switzerland and Minerals*
521 *Named after Swiss Individuals*. Kristallografik Verlag, Achberg, p.130–131.
- 522 Shannon, R.D. (1976) Revised effective ionic radii and systematic studies of interatomic
523 distances in halides and chalcogenides. *Acta Crystallographica*, **32**, 751–767.
- 524 Strunz, H., and Nickel, E.H. (2001) *Strunz Mineralogical Tables. Chemical Structural Mineral*
525 *Classification System*. 9th Ed., 870 pp. Schweizerbart, Stuttgart.
- 526 Sheldrick, G.M. (2008) A short history of SHELX. *Acta Crystallographica*, **A64**, 112–122.
-

- 527 Wilson, A.J.C. (editor) (1992) *International Tables for Crystallography. Volume C:*
528 *Mathematical, physical and chemical tables*. Kluwer Academic Publishers, Dordrecht,
529 The Netherlands.
- 530 Yvon, K., Jeitschko, W., and Parthé, E. (1977) LAZY PULVERIX, a computer program, for
531 calculating X-ray and neutron diffraction powder patterns. *Journal of Applied*
532 *Crystallography*, **10**, 73–74.
-

TABLES

Table 1a.

	Wt.%	Range	SD	Probe standard (line)
Na ₂ O	4.06	3.72-4.22	0.20	albite Amelia (NaK α)
CaO	0.05	0.03-0.06	0.01	diopside (CaK α)
MgO	0.96	0.90-1.01	0.05	synthetic periclase (MgK α)
MnO	41.76	40.94-42.46	0.41	MnTiO ₃ (MnK α)
Mn ₂ O ₃ ***	3.07	2.55-3.87	0.53	
Al ₂ O ₃	0.04	0.01-0.12	0.04	corundum (AlK α)
CuO	0.02	0.01-0.04	0.01	metallic Cu (CuK α)
SiO ₂	39.73	38.70-40.21	0.59	diopside (SiK α)
As ₂ O ₅	6.87	6.10-7.79	0.61	synthetic AsGa (AsL α)
V ₂ O ₅ **	1.43	1.35-1.61	0.11	vanadinite (VK α)
SO ₃	0.01	0.01-0.02	0.01	sphalerite (SK α)
F	0.04	0.00-0.19	0.00	fluorite (FK α)
H ₂ O*	2.20	2.12-2.24		
O = F	-0.02	0.08-0.00		
Total	97.44	96.85-98.26		

Notes: * H₂O calculated in order to have 2(OH) p.f.u.; **total V is reported as V₂O₅ but tetrahedral V⁵⁺ is calculated as 6 – (Si + As), and excess V is assigned to the octahedral sites as V³⁺, following Nagashima and Ambruster (2010a); ***Mn²⁺/Mn³⁺ ratio calculated (Mn³⁺/total Mn = 0.066) in order to obtain 2(OH) groups p.f.u. and V distributed as reported.

Table 1a. Chemical data for braccoite (5 analytical points)

Table 1b.

Wt %	Valletta mine, Italy (1)	Molinello mine, Italy (2)	Ködnitz Valley, Austria (3)
As ₂ O ₅	16.91	16.07	18.35
V ₂ O ₅	0.59	1.67	
Sb ₂ O ₅	0.01		
SiO ₂	31.45	32.38	31.91
TiO ₂			0.02
Al ₂ O ₃			0.02
FeO	-	0.17	0.56
MnO	46.88	48.34	46.02
CaO	0.27	0.75	0.75
MgO	0.39	-	0.00
PbO	0.04		
SO ₃	0.03	-	
Na ₂ O	0.01		0.03
F	0.11		
O=F	0.05		
Total	96.59	99.38	97.66

(1) this work (average of 3 analytical points); (2) Gramaccioli et al. (1980); (3) Albrecht (1990)

Table 1b. Comparison of chemical data available for tiragalloite from other localities.

Table 2.

h	k	l	$d_{\text{obs}}(\text{\AA})$	$d_{\text{calc}}(\text{\AA})$	Int. (obs)	Int. (calc)	h	k	l	$d_{\text{obs}}(\text{\AA})$	$d_{\text{calc}}(\text{\AA})$	Int. (obs)	Int. (calc)
1	4	1	4.785	4.798	8	7.8	2	2	2	2.393	2.399	9	2.3
0	2	0	4.723	4.710	8	10.2	0	4	4	2.388	2.388	22	6.1
2	2	4	3.850	3.842	7	6.1	4	4	4	2.381	2.378	58	18.7
2	4	2	3.836	3.820	21	7.6	0	4	0	2.361	2.355	11	2.9
1	1	1	3.785	3.767	7	6.5	2	2	1	2.283	2.271	12	14.8
0	2	1	3.763	3.741	16	14.7	2	1	4	2.226	2.224	25	13.6
2	2	0	3.741	3.748	9	7.3	0	4	2	2.218	2.223	20	11.3
2	1	2	3.522	3.516	8	1.6	3	4	4	2.204	2.202	21	24.8
0	1	2	3.438	3.420	10	1.1	1	0	4	2.186	2.181	6	4.1
1	2	2	3.337	3.341	19	10.0	2	3	3	2.185	2.172	8	4.5
1	3	0	3.310	3.308	8	8.1	3	4	2	2.091	2.084	9	5.5
1	2	2	3.212	3.192	9	3.5	1	2	4	2.082	2.084	10	14.1
1	4	2	3.143	3.147	19	27.2	3	1	1	2.067	2.060	12	13.9
1	3	4	3.055	3.042	6	2.4	5	4	4	1.779	1.773	7	6.5
2	2	1	3.055	3.064	69	55.4	3	1	2	1.738	1.732	7	7.0
1	3	1	3.054	3.063	17	18.2	1	2	5	1.693	1.694	9	5.5
1	0	2	3.042	3.037	43	15.2	4	5	0	1.680	1.683	24	15.3
3	2	4	3.012	3.010	65	26.9	4	3	-3	1.680	1.676	36	25.9
2	3	0	2.998	3.002	6	4.7	4	2	5	1.655	1.648	14	14.7
2	3	4	2.985	2.979	55	31.5	3	3	3	1.595	1.599	7	5.7
1	0	3	2.974	2.967	8	4.7	0	5	2	1.595	1.586	13	13.7
2	1	3	2.825	2.822	100	100.0	4	0	2	1.545	1.542	7	6.1
2	2	0	2.708	2.696	92	72.7	0	3	5	1.537	1.540	6	5.1
1	1	2	2.699	2.687	6	10.0	5	3	5	1.495	1.488	9	7.8
1	3	0	2.673	2.661	20	10.8	3	4	-6	1.485	1.480	7	2.9
3	0	3	2.655	2.647	12	17.8	6	0	5	1.440	1.436	6	2.4
2	3	2	2.627	2.614	43	29.4	1	0	5	1.434	1.431	15	13.2
0	1	3	2.433	2.422	15	18.1	6	3	0	1.434	1.434	15	12.7

Notes: *Only reflections with $I_{\text{rel}} > 6\sigma(I_{\text{rel}})$ are listed; differences in observed and calculated intensities are related to preferred orientation

Table 2. Observed and calculated X-ray powder diffraction data for braccoite. The ten strongest reflections are reported in bold *

Table 3.

Crystal system	Triclinic
Space group	$P\bar{1}$
Unit-cell dimensions	
a (Å)	9.7354(4)
b (Å)	9.9572(3)
c (Å)	9.0657(3)
α (°)	92.691(2)
β (°)	117.057(4)
γ (°)	105.323(3)
V (Å ³)	740.37(4)
Z	2
μ (mm ⁻¹)	5.62
$F(000)$	758.78
D_{calc} (g cm ⁻³)	3.56
Crystal size (mm)	0.20 × 0.15 × 0.17
Radiation type	MoK α (0.71073 Å)
θ -range for data collection (°)	3.5-32.3
R_{int} (%)	3.13
Reflections collected	18039
Independent reflections	4911
$F_o > 4\sigma(F)$	4389
Refinement method	least-squares matrix: full
No. of refined parameters	300
Final R_{obs} (%) all data	4.14
R_I (%) $F_o > 4\sigma(F)$	3.47
wR_2 (%) $F_o > 4\sigma(F)$	8.61
Highest peak/deepest hole (e ⁻ Å ⁻³)	+0.81 / -0.66
Goodness of fit on F^2	1.191

Table 3. Crystal data and summary of parameters describing data collection and refinement for braccoite

Table 4.

	Site occupancy	x/a	y/b	z/c	U_{iso}
Na(1)	1 Na ⁺	½	0	½	0.0300(5)
Na(2)	0.521(6) Na ⁺	0.1912(3)	0.5340(2)	0.4432(3)	0.0151(7)
Mn(1)	0.953(5) Mn ²⁺ 0.047(5) Mg ²⁺	0.74388(5)	0.97982(5)	0.29542(6)	0.01168(14)
Mn(2)	0.917(5) Mn ²⁺ 0.083(5) Mg ²⁺	0.99723(5)	0.21282(5)	0.22004(6)	0.01045(15)
Mn(3)	0.843(5) Mn ²⁺ 0.157(5) Mg ²⁺	0.86298(5)	0.88807(5)	0.02950(6)	0.00981(16)
Mn(4)	0.944(5) Mn ²⁺ 0.056(5) Mg ²⁺	0.57398(5)	0.66844(4)	0.09774(5)	0.00999(15)
Mn(5)	0.953(5) Mn ²⁺ 0.047(5) Mg ²⁺	0.71912(5)	0.55370(5)	0.85346(6)	0.01242(15)
T(1)	1 Si ⁴⁺	0.87449(9)	0.27556(8)	0.82439(10)	0.00920(15)
T(2)	1 Si ⁴⁺	0.03102(9)	0.23894(8)	0.60955(9)	0.00861(15)
T(3)	1 Si ⁴⁺	0.20746(9)	0.54939(8)	0.77372(10)	0.00943(15)
T(4)	1 Si ⁴⁺	0.47814(9)	0.75745(8)	0.73037(9)	0.00925(15)
T(5)	1 Si ⁴⁺	0.61959(9)	0.07757(8)	0.89560(9)	0.00829(15)
T(6)	0.465(3) Si ⁴⁺ 0.535(3) As	0.60697(5)	0.71401(4)	0.48355(5)	0.00903(12)
O(1)	1 O	0.7048(2)	0.1654(2)	0.7947(3)	0.0132(4)
O(2)	1 O	0.8853(2)	0.2267(2)	0.6567(3)	0.0145(4)
O(3)	1 O	0.1110(2)	0.4094(2)	0.6204(3)	0.0133(4)
O(4)	1 O	0.3022(2)	0.6692(2)	0.7062(3)	0.0124(4)
O(5)	1 O	0.4987(2)	0.9265(2)	0.7529(3)	0.0128(4)
O(6)	1 O	0.4645(2)	0.7114(2)	0.5465(3)	0.0142(4)
O(7)	1 O	0.8556(3)	0.4331(2)	0.8222(3)	0.0144(4)
O(8)	1 O	0.9645(2)	0.7248(2)	0.0081(3)	0.0118(4)
O(9)	1 O	0.9535(2)	0.1532(2)	0.4220(2)	0.0123(4)
O(10)	1 O	0.8287(2)	0.8130(2)	0.2469(2)	0.0110(4)
O(11)	1 O	0.0805(2)	0.6058(2)	0.8035(3)	0.0143(4)
O(12)	1 O	0.6649(2)	0.4918(2)	0.0594(2)	0.0114(4)
O(13)	1 O	0.3746(2)	0.2765(2)	0.1181(2)	0.0113(4)
O(14)	1 O	0.4961(2)	0.1480(2)	0.9102(3)	0.0127(4)
O(15)	1 O	0.2404(2)	0.9490(2)	0.9367(2)	0.0112(4)
O(16)	1 O	0.6809(3)	0.8807(2)	0.4750(3)	0.0148(4)
O(17)	1 O	0.5172(2)	0.6042(2)	0.2977(3)	0.0137(4)
O(18)	1 O	0.2568(3)	0.3469(2)	0.3699(3)	0.0149(4)
O(19)	1 O	0.0897(2)	0.0502(2)	0.1728(3)	0.0134(4)
H(7)	1 H	0.937(5)	0.493(4)	0.820(5)	0.017***
H(19)**	1 H	0.179(3)	0.050(4)	0.276(3)	0.016***

Notes: *The temperature factor has the form $\exp(-T)$ where $T = 8 (\pi^2) U(\sin(\theta)/\lambda)^2$ for isotropic atoms.

Atom coordinates refined with a soft constraint to O-H of 0.98 Å, * U_{iso} refined constrained to be 1.2 the isotropic equivalent of the oxygen atom of the hydroxyl group

Table 4. Multiplicities, fractional atom coordinates, and equivalent isotropic displacement parameters (Å²) for braccoite*

Table 5.

	U_{11}	U_{22}	U_{33}	U_{12}	U_{13}	U_{23}
Na(1)	0.0487(13)	0.0380(12)	0.0215(10)	0.0280(10)	0.0230(10)	0.0175(9)
Na(2)	0.0233(13)	0.0130(12)	0.0087(11)	0.0032(9)	0.0090(10)	0.0023(8)
Mn(1)	0.0098(2)	0.0107(2)	0.0128(2)	0.00149(16)	0.00516(17)	0.00090(16)
Mn(2)	0.0103(2)	0.0107(2)	0.0104(2)	0.00265(16)	0.00545(17)	0.00342(16)
Mn(3)	0.0098(2)	0.0093(2)	0.0112(2)	0.00304(17)	0.00566(18)	0.00310(16)
Mn(4)	0.0093(2)	0.0091(2)	0.0111(2)	0.00244(16)	0.00485(17)	0.00261(15)
Mn(5)	0.0125(2)	0.0113(2)	0.0153(2)	0.00397(17)	0.00813(18)	0.00284(16)
T(1)	0.0087(3)	0.0102(3)	0.0101(3)	0.0031(3)	0.0055(3)	0.0040(3)
T(2)	0.0085(3)	0.0092(3)	0.0079(3)	0.0025(3)	0.0039(3)	0.0027(3)
T(3)	0.0086(3)	0.0088(3)	0.0110(3)	0.0021(3)	0.0050(3)	0.0039(3)
T(4)	0.0097(3)	0.0090(3)	0.0093(3)	0.0025(3)	0.0049(3)	0.0038(3)
T(5)	0.0081(3)	0.0091(3)	0.0086(3)	0.0029(3)	0.0044(3)	0.0038(3)
T(6)	0.0098(2)	0.00979(19)	0.00859(19)	0.00275(14)	0.00542(15)	0.00280(13)
O(1)	0.0107(9)	0.0153(9)	0.0142(9)	0.0024(7)	0.0072(8)	0.0071(8)
O(2)	0.0118(9)	0.0220(10)	0.0113(9)	0.0053(8)	0.0069(8)	0.0043(8)
O(3)	0.0159(10)	0.0102(9)	0.0104(9)	0.0016(7)	0.0049(8)	0.0020(7)
O(4)	0.0112(9)	0.0131(9)	0.0129(9)	0.0020(7)	0.0065(7)	0.0052(7)
O(5)	0.0138(9)	0.0087(8)	0.0121(9)	0.0012(7)	0.0045(8)	0.0036(7)
O(6)	0.0129(9)	0.0199(10)	0.0099(9)	0.0037(8)	0.0064(8)	0.0032(8)
O(7)	0.0134(10)	0.0108(9)	0.0214(11)	0.0042(8)	0.0101(8)	0.0058(8)
O(8)	0.0112(9)	0.0132(9)	0.0112(9)	0.0056(7)	0.0046(7)	0.0034(7)
O(9)	0.0137(9)	0.0134(9)	0.0087(9)	0.0022(7)	0.0056(7)	0.0019(7)
O(10)	0.0107(9)	0.0121(9)	0.0091(9)	0.0040(7)	0.0036(7)	0.0023(7)
O(11)	0.0148(10)	0.0140(9)	0.0200(10)	0.0063(8)	0.0120(8)	0.0069(8)
O(12)	0.0115(9)	0.0114(9)	0.0103(9)	0.0035(7)	0.0044(7)	0.0038(7)
O(13)	0.0128(9)	0.0120(9)	0.0103(9)	0.0051(7)	0.0059(7)	0.0040(7)
O(14)	0.0128(9)	0.0140(9)	0.0142(9)	0.0062(7)	0.0078(8)	0.0047(7)
O(15)	0.0115(9)	0.0110(9)	0.0104(9)	0.0034(7)	0.0048(7)	0.0044(7)
O(16)	0.0175(10)	0.0130(9)	0.0136(10)	0.0031(8)	0.0081(8)	0.0048(8)
O(17)	0.0142(9)	0.0142(9)	0.0105(9)	0.0017(8)	0.0060(8)	0.0003(7)
O(18)	0.0133(9)	0.0159(10)	0.0165(10)	0.0068(8)	0.0066(8)	0.0069(8)
O(19)	0.0125(9)	0.0153(9)	0.0112(9)	0.0049(8)	0.0044(8)	0.0034(7)

Notes: * The temperature factor has the form $\exp(-T)$ where $T = 2\pi^2 \sum_{ij} (h(i)h(j)U(i,j)a^*(i)a^*(j))$.

Table 5. Anisotropic displacement parameters for braccoite (\AA)*

Table 6.

Na(1) - O(5) (×2)	2.444(2)	Mn(2) - O(11)	2.119(2)	Mn(5) - O(7)	2.108(2)	T(3) - O(11)	1.604(2)	T(6) - O(16)	1.646(2)
- O(16) (×2)	2.451(2)	- O(9)	2.136(2)	- O(17)	2.159(2)	- O(12)	1.618(2)	- O(17)	1.667(2)
- O(1) (×2)	2.613(2)	- O(19)	2.161(2)	- O(13)	2.178(2)	- O(4)	1.628(2)	- O(18)	1.670(2)
- O(6) (×2)	<u>2.877(2)</u>	- O(15)	2.189(2)	- O(12)	2.231(2)	- O(3)	<u>1.642(2)</u>	- O(6)	<u>1.719(2)</u>
<Na(1) - O>	2.596	- O(18)	2.222(2)	- O(8)	2.270(2)	<T(3) - O>	1.623	<T(6) - O>	1.675
** $V(\text{Å}^3)$	26.007	- O(8)	<u>2.346(2)</u>	- O(18)	<u>2.374(2)</u>	$V(\text{Å}^3)$	2.188	$V(\text{Å}^3)$	2.403
		<Mn(2) - O>	2.196	<Mn(5) - O>	2.220	σ^{2*}	7.846	σ^{2*}	12.945
Na(2) - O(18)	2.285(3)	$V(\text{Å}^3)$	13.711	$V(\text{Å}^3)$	14.066	λ^*	1.0019	λ^*	1.0032
- O(4)	2.292(3)	σ^{2*}	67.545	σ^{2*}	86.772				
- O(7)	2.293(3)	λ^*	1.0207	λ^*	1.0260	T(4) - O(13)	1.602(2)		
- O(3)	2.355(3)					- O(4)	1.612(2)		
- O(6)	2.484(3)	Mn(3) - O(19)	2.116(2)	T(1) - O(8)	1.613(2)	- O(5)	1.633(2)		
- O(11)	2.513(3)	- O(8)	2.156(2)	- O(1)	1.617(2)	- O(6)	<u>1.643(2)</u>		
- O(2)	2.753(3)	- O(19)	2.163(2)	- O(7)	1.626(2)	<T(4) - O>	1.623	H(7) - O(7)	0.86(4)
- O(3)	<u>2.944(3)</u>	- O(13)	2.191(2)	- O(2)	<u>1.632(2)</u>	$V(\text{Å}^3)$	2.181	H(7) ... O(11)	1.62(4)
<Na(2) - O>	2.490	- O(15)	2.199(2)	<T(1) - O>	1.622	σ^{2*}	14.064	O(7) ... O(11)	2.48(1)
$V(\text{Å}^3)$	25.210	- O(10)	<u>2.272(2)</u>	$V(\text{Å}^3)$	2.178	λ^*	1.0033	O(7)- H(7)...O(11)	176.37(2)°
		<Mn(3) - O>	2.183	σ^{2*}	15.761				
Mn(1) - O(9)	2.069(2)	$V(\text{Å}^3)$	13.523	λ^*	1.0038	T(5) - O(14)	1.592(2)	H(19) - O(19)	0.95(2)
- O(10)	2.150(2)	σ^{2*}	55.177			- O(15)	1.607(2)	H(19) ... O(16)	1.99(2)
- O(16)	2.177(2)	λ^*	1.0174	T(2) - O(9)	1.596(2)	- O(1)	1.634(2)	O(19) ... O(16)	2.855(10)
- O(14)	2.190(2)			- O(10)	1.626(2)	- O(5)	<u>1.679(2)</u>	O(19)- H(19)...O(16)	150.34(18)°
- O(15)	2.308(2)	Mn(4) - O(14)	2.107(2)	- O(2)	1.635(2)	<T(5) - O>	1.628		
- O(5)	<u>2.627(2)</u>	- O(12)	2.190(2)	- O(3)	<u>1.647(2)</u>	$V(\text{Å}^3)$	2.183		
<Mn(1) - O>	2.253	- O(17)	2.199(2)	<T(2) - O>	1.626	σ^{2*}	41.722		
$V(\text{Å}^3)$	14.087	- O(10)	2.220(2)	$V(\text{Å}^3)$	2.200	λ^*	1.0098		
σ^{2*}	170.515	- O(12)	2.246(2)	σ^{2*}	9.140				
λ^*	1.0617	- O(13)	<u>2.287(2)</u>	λ^*	1.0021				
		<Mn(4) - O>	2.208						
		$V(\text{Å}^3)$	13.939						
		σ^{2*}	67.478						
		λ^*	1.0204						

Notes: *Mean quadratic elongation (λ) and the angle variance (σ^2) were computed according to Robinson *et al.* (1971); ** V = polyhedral volume

Table 6. Main interatomic distances (Å) and geometrical parameters for braccoite

Table 7.

	T(1)	T(2)	T(3)	T(4)	T(5)	T(6)	M(1)	M(2)	M(3)	M(4)	M(5)	Na(1)	Na(2)	H(7)	H(19)		+ H contrib
O(1)	1.013				0.968							0.115 × 2 [↓]				2.096	
O(2)	0.975	0.965											0.047			1.987	
O(3)		0.937	0.949										0.116			2.032	
O(4)				0.985	1.026								0.030			2.145	
[IV]O(5)				0.972	0.863		0.120					0.169 × 2 [↓]				2.123	
[IV]O(6)				0.946		1.029						0.063 × 2 [↓]	0.086			2.124	
[IV]O(7)	0.988										0.409		0.133	1.019		1.531	2.550
[IV]O(8)	1.024							0.223	0.353		0.271			0.475		1.871	2.006
O(9)		1.073					0.457	0.376								1.906	
[IV]O(10)		0.988					0.369		0.264	0.306						1.928	
[IV]O(11)			1.050					0.393						0.081	0.255	1.524	1.779
														0.475		1.999	
O(12)			1.010							0.331	0.298					1.927	
[IV]O(13)				1.056					0.323	0.260	0.341					1.980	
O(14)					1.084		0.332			0.410						1.826	
[IV]O(15)					1.041		0.248	0.328	0.317							1.934	
[IV]O(16)						1.240	0.344					0.166 × 2 [↓]			0.162	1.749	1.911
O(17)						1.173				0.323	0.358					1.855	
[IV]O(18)						1.167		0.302			0.211		0.136			1.815	
O(19)								0.353	0.392						0.824	1.091	1.915
									0.347								
	4.000	3.963	3.994	3.999	3.956	4.609	1.870	1.975	1.996	1.917	1.888	1.026	0.763	1.274	0.986		37.38
														0.950			
F.C.*	4.000	4.000	4.000	4.000	4.000	4.630	2.000	2.070	2.240	2.030	2.000	1.000	0.560	1.000	1.000	37.96	

Note: anion sites coordination reported only for coordination other than 3. * F.C. = formal charge at site on the basis of chemical formula

Table 7. Bond valence calculations for braccoite (Brown, 1981)

Table 8.

Site	Refined site-scattering (<i>apfu</i>)	Assigned site-population	Calculated site-scattering (<i>epfu</i>)	$\langle X-\varphi \rangle_{\text{calc.}}^*$ (Å)	$\langle X-\varphi \rangle_{\text{obs.}}$ (Å)	Ideal composition (<i>apfu</i>)
Cations						
<i>Mn</i> (1)	24.39(7)	0.98 Mn ²⁺ + 0.01 Mg + 0.01 Ca	24.82	2.191	2.253	Mn ²⁺
<i>Mn</i> (2)	23.93(7)	0.87 Mn ²⁺ + 0.07 Mn ³⁺ + 0.06 Mg	24.22	2.170	2.196	Mn ²⁺
<i>Mn</i> (3)	22.96(7)	0.56 Mn ²⁺ + 0.32 Mn ³⁺ + 0.10 Mg + 0.01 V ³⁺ + 0.01 Al ³⁺ +	23.53	2.130	2.183	Mn ²⁺
<i>Mn</i> (4)	24.28(7)	0.96 Mn ²⁺ + 0.03 Mn ³⁺ + 0.01 Mg	24.87	2.183	2.208	Mn ²⁺
<i>Mn</i> (5)	24.39(7)	0.99 Mn ²⁺ + 0.01 Mg	24.87	2.189	2.220	Mn ²⁺
<i>T</i> (6)	24.17(6)	0.48 As + 0.37 Si + 0.15 V ⁵⁺	24.47	1.671	1.675	As
<i>Na</i> (1)	11	1.00 Na	11.00	2.560	2.596	Na**
<i>Na</i> (2)	5.72(6)	0.56 Na + 0.44 □	6.16	2.560	2.490	Na, □
Anions						
^[IV] O(19)		0.98 OH + 0.02 F				OH

X = cation, φ = O, OH, F;

* calculated by summing constituent ionic radii; values from Shannon (1976);

** site in special position, half multiplicity;

Table 8. Refined site-scattering and assigned site-populations for braccoite

Table 9.

	Braccoite	Saneroite	Scheuchzerite	Steedeite
Reference	(1)	(2, 3)	(4)	(5)
Formula	$\text{NaMn}^{2+}_5[\text{Si}_5\text{AsO}_{17}(\text{OH})](\text{OH})$	$\text{NaMn}^{2+}_5[\text{Si}_5\text{VO}_{17}(\text{OH})](\text{OH})$	$\text{NaMn}^{2+}_9[\text{Si}_9\text{O}_{25}(\text{OH})(\text{VO}_3)](\text{OH})$	$\text{NaMn}_2[\text{Si}_3\text{BO}_9](\text{OH})_2$
Crystal system	Triclinic	Triclinic	Triclinic	Triclinic
Space group	$P\bar{4}$	$P\bar{4}$	$P\bar{4}$	$P\bar{4}$
a (Å)	9.7354(4)	9.741(5)	9.831(5)	6.837(1)
b	9.9572(3)	9.974(7)	10.107(5)	7.575(2)
c	9.0657(3)	9.108(5)	13.855(7)	8.841(2)
α (°)	92.691(2)	92.70(4)	86.222(10)	99.91(3)
β	117.057(4)	117.11(4)	73.383(9)	102.19(3)
γ	105.323(3)	105.30(4)	71.987(9)	102.78(3)
V (Å ³)	740.37(4)	744.16	1254.2(10)	424.81(1)
Z	2	2	2	2
Axial ratios ($a:b:c$)	0.978:1:0.910	0.977:1:0.913	0.973:1:1.371	0.9026:1:1.1671
D_{meas} (g cm ⁻³)	n.d.	3.47	3.50(2)	n.d.
D_{calc} (g cm ⁻³)	3.56	3.51	3.47	3.104
Strongest lines in the powder pattern: d_{obs} (Å)(l)	3.774(30), 3.514(30), 3.042(60), 3.005(60), 2.973(80), 2.821(100), 2.696(90), 2.620(30), 2.676(50), 1.673(30)	3.06(s), 2.83(s), 2.70(s), 3.01(m), 2.98(m), 2.62(m), 2.20(m)	2.71(100), 3.09(80), 7.91(70), 8.68(50), 2.92(40), 3.22(40), 3.94(30), 4.83(30)	8.454 (100), 7.234(39), 3.331(83), 3.081(38), 2.859(52), 2.823(80)
Optical character	biaxial (+)	biaxial (-)	biaxial (+)	biaxial
Colour	brown-red	bright orange	yellow-orange	pale pink to colourless
Pleochroism	X = brownish yellow, Y = dark yellow, Z = yellow	X = deep orange; Y = lemon- yellow; Z = yellow-orange	X = brown yellow; Y = pale yellow	Not observed
Hardness (Mohs)	n.d.	n.d.	2-3	n.d.
Streak	pale-yellow	white	yellow-orange	white
Luster	vitreous to resinous	resinous to greasy	vitreous	vitreous
Habit and forms	subhedral	tabular-prismatic crystals	acicular and prismatic crystals	acicular crystals
Association	aegirine, hematite, tiragalloite, quartz, unidentified Mn oxides, and Mn silicates	quartz, baryte, caryopilite, ganophyllite, medaite, palenzonaite, pyrobelonite, fianelite, parsettensite, rhodochrosite, kutnahorite, aegirine	saneroite, tiragalloite	aegirine, analcime, catapleiite, eudialyte, microcline nepheline, natrolite, pyrrhotite, sérandite, sodalite, thermonatrite

Refs: (1) this work; (2) Lucchetti *et al.* (1981); (3) Nagashima and Armbruster (2010a); (4) Brugger *et al.* (2006); (5) Haring and McDonald (2014).

Table 8. Comparison of minerals related to braccoite. References are given in brackets

Table 9.

	Saneroite (Molinello mine, Italy) ¹				Saneroite (Fianel, Switzerland) ¹		Braccoite (Valletta mine, Italy) ²	
	specimen 1		specimen 2		Wt%	SD	Wt%	SD
	Wt%	SD	Wt%	SD				
SiO ₂	39.99	1.06	39.06	0.65	41.03	0.98	39.73	0.59
Al ₂ O ₃	0.02	0	0.01	0.02	0.01	0.02	0.04	0.04
MnO	42.2	1.38	40.33	1.06	41.53	1.12	39.00	0.41
Mn ₂ O ₃	-	-	-	-	-	-	3.07	0.53
MgO	0.01	0.02	0.00	0.00	0.03	0.04	0.96	0.05
CaO	0.13	0.05	0.11	0.04	0.33	0.12	0.05	0.01
Na ₂ O	4.34	0.28	4.36	0.27	4.52	0.25	4.06	0.2
K ₂ O	0	0.01	0.01	0.01	0.01	0.01	-	-
CuO	0.1	0.14	0.2	0.24	0.14	0.2	0.02	0.01
NiO	0.03	0.04	0.03	0.03	0.02	0.03	-	-
V ₂ O ₅	7.15	1.8	7.78	0.7	6.05	1.23	1.43	0.11
As ₂ O ₅	1.22	1.27	1.92	1.65	1.31	1.85	6.87	0.61
SO ₃	-	-	-	-	-	-	0.01	0.01
F	-	-	-	-	-	-	0.04	0
Total	95.19		93.81		94.98		95.28	

Refs: (1) Nagashima and Armbruster, 2010a; (2) this work

Table 9. Comparison of chemical data between saneroite from Molinello mine (Italy) and Fianel (Switzerland) and braccoite from Valleta (this work).

FIGURE CAPTIONS

Figure 1. a) Picture of the rocks containing braccoite; b) Picture of rare red crystalline masses with brown hue of braccoite holotype intergrown with orange tiragalloite forming a thin layer on hematite and quartz (FoV: 5 mm). Photo of R. Bracco.

Figure 2. BSE image of a section of a quartz (qtz) vein showing braccoite (brac) and tiragalloite (tirag) used during the WDS analyses. Small spot within quartz is baryte (bary)

Figure 3. Raman spectra of braccoite in the 200-4000 cm^{-1} region and between 200 and 1200 cm^{-1} .

Figure 4. Raman spectra of tiragalloite in the 150-4000 cm^{-1} region and between 150 and 1200 cm^{-1} .

Figure 5. Detail of the braccoite structure showing the bands of Mn octahedra and the silicate chains. Blue: Si tetrahedra; green: As-Si tetrahedron; yellow: Mn octahedra; light blue: Na.; white: H. Violet double arrow shows the short $Na(2)\dots H(7)$ distance. Approx. vector of projection is [545]. Design obtained with Vesta 3 (Momma and Izumi, 2011).

Figure 1a.



Figure 1b.

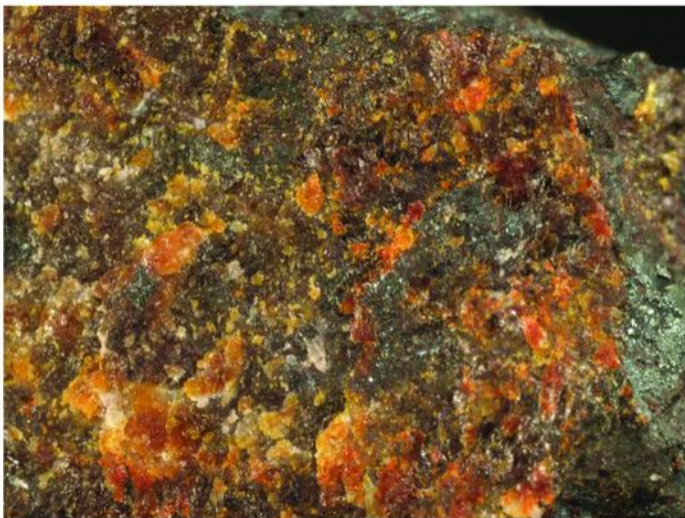


Figure 2.

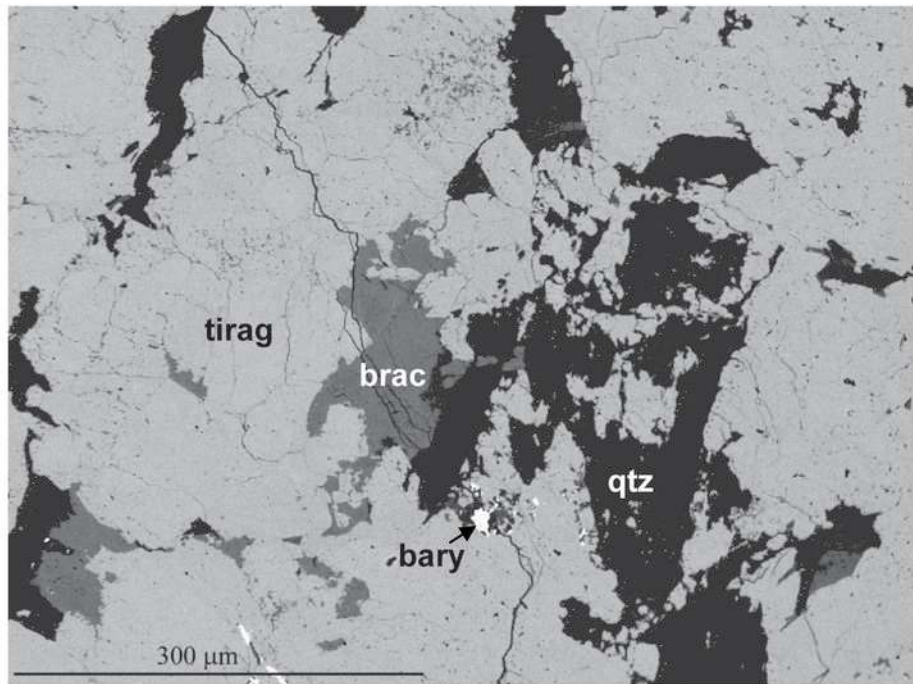


Figure 3.

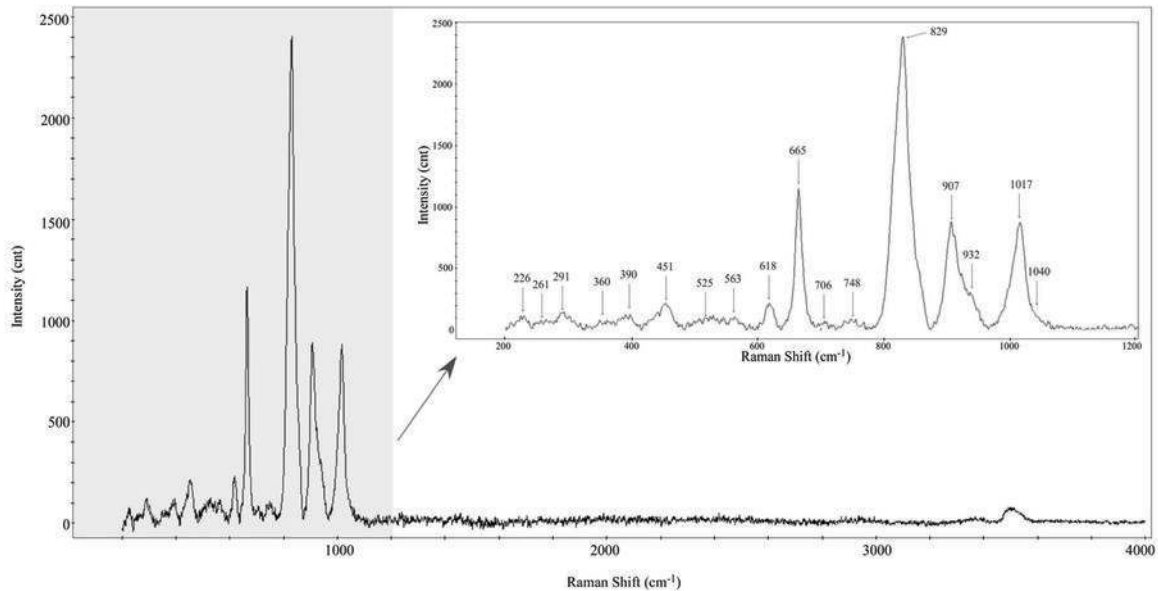


Figure 4.

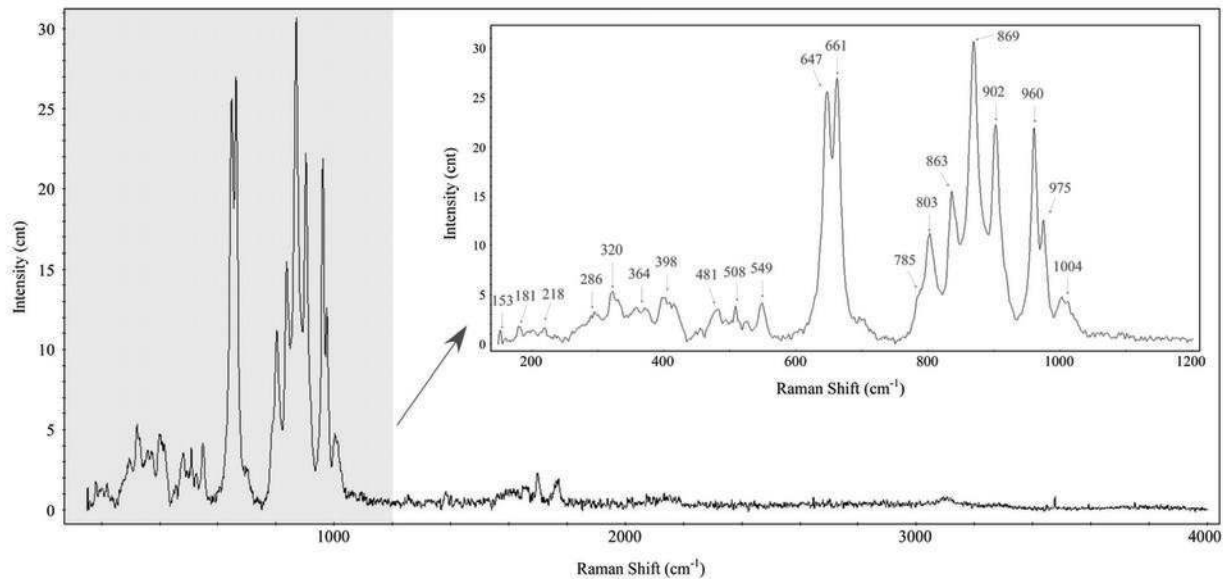


Figure 5.

